Published in final edited form as:
Biochem J. 2012 September 15; 446(3): 455–467. doi:10.1042/BJ20111961.

NOVEL ATYPICAL PKC INHIBITORS PREVENT VASCULAR ENDOTHELIAL GROWTH FACTOR-INDUCED BLOOD-RETINAL BARRIER DYSFUNCTION

Paul M. Titchenell[1,*,‡], **Cheng-Mao Lin**[†], **Jason M. Keil**[†], **Jeffrey M. Sundstrom**[‡], **Charles D. Smith**[§], and **David A. Antonetti**[†]

[*]Department of Cellular and Molecular Physiology, Penn State University College of Medicine, Hershey, PA 17033, USA

[†]Department of Ophthalmology and Visual Sciences, The University of Michigan Kellogg Eye Center, Ann Arbor, MI 48108, USA

[‡]Department of Ophthalmology, Penn State University College of Medicine, Hershey, PA 17033, USA

[§]Department of Pharmaceutical Sciences, Medical University of South Carolina, Charleston, SC 29425, USA

SYNOPSIS

Pro-inflammatory cytokines and growth factors such as vascular endothelial growth factor (VEGF) contribute to the loss of the blood-retinal barrier (BRB) and subsequent macular edema in various retinal pathologies. VEGF signaling requires conventional PKC (PKCβ) activity; however, PKCβ inhibition only partially prevents VEGF-induced endothelial permeability and does not affect pro-inflammatory cytokine-induced permeability suggesting the involvement of alternative signaling pathways. Here, we provide evidence for the involvement of atypical protein kinase C (aPKC) signaling in VEGF-induced endothelial permeability and identify a novel class of inhibitors of aPKC that prevent BRB breakdown *in vivo*. Genetic and pharmacological manipulations of aPKC isoforms were used to assess their contribution to endothelial permeability in culture. A chemical library was screened using an *in vitro* kinase assay to identify novel small molecule inhibitors and further medicinal chemistry was performed to delineate a novel pharmacophore. We demonstrate that aPKC isoforms are both sufficient and required for VEGF-induced endothelial permeability. Furthermore, these specific, potent, non-competitive, small molecule inhibitors prevented VEGF-induced tight junction internalization and retinal endothelial permeability in response to VEGF in both primary culture and in rodent retina. These data suggest that aPKC inhibition with 2-amino-4-phenyl-thiophene derivatives may be developed to preserve the BRB in retinal diseases such as diabetic retinopathy or uveitis and the blood-brain barrier (BBB) in the presence of brain tumors.

Keywords

vascular endothelial growth factor (VEGF); atypical protein kinase C (aPKC); blood-retinal barrier (BRB); blood-brain barrier (BBB)

[1]Address correspondence to: Paul M. Titchenell, The Pennsylvania State University College of Medicine, Hershey, 17033 USA. Tel: +1 717-531-5542; pmt132@psu.edu.

AUTHOR CONTRIBUTIONS

P.M.T. researched data, contributed to discussion, and wrote the manuscript. J.M.S. contributed to discussion and reviewed/edited the manuscript. J.M.K., C.-M.L., C.D.S., and D.A.A. researched data, contributed to discussion, and reviewed/edited the manuscript.

INTRODUCTION

The blood-brain and blood-retinal barriers require a well-developed tight junction (TJ) complex in the vascular endothelium to create the defined environment required for proper neuronal function. In retinal pathologies such as age-related macular degeneration (AMD), diabetic macular edema (DME), retinopathy of prematurity (ROP), and retinal vein occlusions (RVO) breakdown of the vascular endothelial TJ complex leads to vessel hyper-permeability, tissue edema and loss of neural function [1-4]. Growth factors such as VEGF and pro-inflammatory cytokines such as TNFα have been implicated in the pathophysiology of these diseases and directly contribute to the retinal vascular hyper-permeability, angiogenesis, and inflammation that are clinically observed. [5-9]. Indeed, antibodies to VEGF improve visual function in patients undergoing laser surgery for diabetic macular edema; however, this was only observed in ~50% patients [10-12]. These results suggest a need for the identification of downstream regulators of BRB dysfunction and the elucidation of common mechanisms associated with growth factor and pro-inflammatory cytokine signaling may provide an ideal therapeutic target.

Previous studies have focused on the role of classical PKC isoforms (cPKCs), and PKCβ in particular, in regulating VEGF-induced vascular permeability [13-15]. Endothelial permeability involves VEGF activation of PKCβ leading to phosphorylation and reorganization of the tight junction (TJ) complex increasing vessel wall permeability [16-18]. Recent reports have demonstrated that VEGF increases the phosphorylation of the TJ protein occludin at multiple sites [19] including Ser490 [20] in a PKCβ dependent manner [21]. Phosphorylation at Ser490 allows subsequent ubiquitination and endocytosis of occludin and breaks in the tight junction [20, 22]. However, the PKCβ, inhibitor ruboxistaurin failed to achieve FDA approval for diabetic retinopathy and endothelial cell culture studies demonstrate that inhibition of cPKC isoforms only partially attenuate the VEGF-induced endothelial permeability [19]. Furthermore, cPKC inhibition fails to prevent TNFα-induced permeability [23], a pro-inflammatory cytokine known to contribute to diabetic retinopathy [8, 24] and uveitis [25]. Therefore, elucidation of novel kinases that regulate vascular permeability downstream of growth factors and inflammatory cytokines may provide the optimal therapeutic targets for macular edema associated with a wide range of ophthalmic disease.

The PKC serine/threonine kinases are members of the AGC super family and may be subdivided into three classes. The cPKCs require calcium and DAG for activation and include PKC α, βI/II, and γ. The novel PKC isoforms (nPKCs) include δ, ε, η, θ and require only DAG for activation while the aPKCs, PKC λ(mouse)/ι(human) and ζ, require neither calcium nor DAG for activation [26]. Activation of PKCζ/ι may occur by phosphorylation of two residues at the C-terminus, Thr410/Thr412 and Thr560/Thr555 for PKCζ/ι, respectively [27]. Activation of phosphatidylinositol 3-kinase pathway leads to PH domain dependent kinase 1 (PDK1) activation that can directly phosphorylate Thr410/Thr412 on PKCζ/ι liberating the pseudosubstrate domain and allowing autophosphorylation of Thr560/Thr555, which results in a fully active kinase [28].

Here, we report the requirement of aPKCs in VEGF-induced endothelial permeability. Additionally, we identify a class of small molecule, non-competitive and specific aPKC inhibitors based on a phenyl-thiophene structural backbone. Altering aPKC isoform activity and content using overexpression and RNAi-mediated knockdown experiments coupled with pseudosubstrate peptide inhibition and the use of novel small molecule inhibitors demonstrate the requirement for aPKC to mediate VEGF-induced permeability in primary cell culture and the rodent retina. Furthermore, a recent report demonstrates the

effectiveness of aPKC inhibition in preventing TNFα-induced retinal endothelial permeability [23]. Therefore, this new class of compounds may lead to the development of novel drugs that preserve the BRB by preventing vascular hyper-permeability in diseases associated with increased VEGF and TNFα expression including diabetic retinopathy, uveitis, and macular degeneration.

EXPERIMENTAL

Reagents

Recombinant human $VEGF_{165}$ was purchased from R&D Systems (Minneapolis, MN, USA). PKCζ/ι myristoylated pseudosubstrate inhibitor was purchased from Calbiochem (Gibbstown, NJ, USA). Small molecules were purchased from ChemBridge Corporation (San Diego, CA, USA), Sigma-Aldrich (St. Louis, MO, USA) or synthesized by Apogee, Inc. (Hershey, PA, USA). The LIVE/Dead viability kit (Invitrogen, Carlsbad, CA, USA) was used to assess cell viability, according to manufacturer's instructions.

Primary Retinal Endothelial Cell (REC) Culture

Primary bovine retinal endothelial cells (BREC) were isolated and cultured from fresh bovine eye tissue as previously described [29]. Human retinal endothelial cells (HREC) were from Cell Systems (Krikland, WA, USA). For experimentation, RECs were grown to confluence and stepped down in 0% FBS or 1% FBS, for 24 h with 100 nM hydrocortisone and treated with VEGF at 50 ng/ml where indicated. All experiments were performed with cells at passage 4-8.

Animals

Male Sprague-Dawley rats (Charles River Laboratories, Wilmington, MA, USA) weighing 150 to 175 g were used to evaluate retinal vascular permeability and tight junction protein localization. Animals were housed under a 12-hour light/dark cycle with free access to water and a standard rat chow. All experiments were conducted in accordance with the Association for Research in Vision and Ophthalmology (ARVO) Statement for the Use of Animals in Ophthalmic and Vision Research, and were approved and monitored by the Institutional Animal Care and Use Committee (IACUC) at the Penn State College of Medicine.

In vitro Permeability Assay

The permeability assay was performed as described previously [30]. The rate of flux of the substrate, Po, was calculated over the 4 hr time course from the following formula [30].

$$P_o = [(F_L/\Delta t)\, V_A] / (F_A A)$$

where P_o is in centimeters per second; F_L is basolateral fluorescence; F_A is apical fluorescence; Δt is change in time; A is the surface area of the filter; and V_A is the volume of the basolateral chamber.

Overexpression of aPKC in primary retinal endothelial cells

BREC were transfected with the aPKC expression plasmid containing PKCζ isoform (pCMV-aPKCζ), gift from Dr. A. Toker, using the nucleofection technique (Lonza, Basel, Switzerland) [19]. Alternatively, BREC were transduced with adenovirus at 90% confluence on transwell filters with AdGFP (vector), a gift from Dr. S. Abcouwer, wild-type aPKC containing PKCζ isoform (AdWTaPKCζ), kinase-dead aPKC containing PKCζ isoform with

a K281W mutation (AdKDaPKCζ), and constitutively active aPKC containing PKCζ isoform with a N-terminal c-src myristoylation signal (AdCAaPKCζ), gifts from Dr. A. Garcia-Ocaña. Adenoviral transduction, which has been shown to successfully transduce primary bovine retinal endothelial cells [23], was performed at a MOI@10,000-20,000 to match expression levels of transgene.

RNAi-mediated knockdown of aPKC isoforms in primary retinal endothelial cells

siRNAs (siGENOME) were designed and purchased from Dharmacon Inc. (Lafayette, CO, USA) using accession number NM_001205955.1 (PKCι) and NM_001077833 (PKCζ) and transfected into BREC at 100 nM using the nucleofection technique (Lonza, Basel, Switzerland) [19]. *In vitro* permeability assay was performed at 72 h following transfection according to aforementioned procedure. The oligonucleotides used were as followed: PKCζ Construct A 5'-CCAUGAAGGUGGUAAAGAA-3', PKCζ Construct B 5'-UGUAAUGUCCCGAGGAAUA-3', PKCι Construct A 5'-GCAAUGAACACCAGGGAAA-3', PKCι Construct B 5'-CUGUAAAAGUCAAUGGUUA-3', PKCι Construct C 5'-AGAAAUCAGUCUAGCAUUA-3', PKCι Construct D 5'-UCCUUCAAGUCAUGAGAGU-3', and Non-Targeting #3 siGENOME (Scramble).

aPKC isoform differentiation and profiling

RNA was isolated from BREC using the RNEasy Kit (Qiagen, Valencia CA, USA) and cDNA was generated using the Verso cDNA Kit (Thermo Scientific, Waltham, MA, USA). PCR was performed using Phusion II High Fidelity Polymerase (NEB, Ipswich, MA, USA). A 470 base pair amplicon was generated with primers 5'-GATGAGGATATTGACTGG-3' and 5'-CCTGCCATCATCTC-3', amplifying both PKCι and PKCζ cDNA. The restriction enzymes Pst1 (PKCι specific) and Stu1 (PKCζ specific) were used to differentiate between aPKC isoforms.

Cell Lysis and Immunoblot Analysis

Cells were harvested in lysis buffer [20] and protein extracts were blotted utilizing the NuPAGE system (Invitrogen, Carlsbad, CA, USA) [31]. Membranes were immunoblotted using anti-Flag (Cell Signaling, Danvers, MA, USA), anti-HA (Cell Signaling, Danvers, MA, USA), anti-pERK1/2 (Cell Signaling, Danvers, MA, USA), anti-ERK1/2 (Cell Signaling, Danvers, MA, USA), anti-pS473 AKT (Cell Signaling, Danvers, MA, USA), anti-AKT (Cell Signaling, Danvers, MA, USA), anti-GFP (Abcam, Cambridge, MA, USA), anti-pThr410/Thr412 PKCζ/ι (Cell Signaling, Danvers, MA, USA), anti-phospho Thr560/Thr555 PKCζ/ι (Abcam, Cambridge, MA, USA), anti-aPKC (C-20) or (H-1) (Santa Cruz, Santa Cruz, CA, USA), and anti-actin (Millipore, Billerica, MA, USA) antibodies. Primary antibodies were detected by anti-rabbit horseradish peroxidase-conjugated IgG with ECL Advance (GE Healthcare, Piscataway, NJ, USA) or anti-mouse alkaline phosphatase-conjugated IgG with ECF (GE Healthcare, Piscataway, NJ, USA).

Immunoprecipitation

Male Sprague-Dawley rats (Charles River Laboratories, Wilmington, MA, USA) were anesthetized with ketamine and xylazine (66.7mg and 6.7mg/kg body weight, intramuscular), and a 32-gauge needle was used to create a hole for an intra-vitreal injection (2.5μl/eye) using a 5-μl Hamilton syringe. Animals received an intra-vitreal injection of either vehicle (0.1% BSA/PBS) or VEGF (50ng) for time indicated. Retinas were excised and lysed in (1% Nonidet P-40, 10% glycerol, 50 mm Tris, pH 7.5, 150 mm NaCl, 2 mm EDTA, 1 mm $NaVO_4$, 10 mm sodium fluoride, 10 mm sodium pyrophosphate, 1 mm benzamidine, complete protease inhibitor mixture). The lysate was centrifuged at 14,000 × *g*

for 10 min, and the supernatant was transferred to another microcentrifuge tube. 750 ug of protein was subjected to a preclear with 100 μl of 1:1 slurry of Protein G-Sepharose™ 4 Fast Flow (GE Healthcare) for 1 h, after brief micro-centrifugation the supernatant was incubated with 5 ug aPKC Ab (C-20) for 2 h. Protein G beads were added, followed by further incubation for 1 h. The beads were recovered by centrifugation at 1500 × *g* for 1 min and washed four times with 1 ml of lysis buffer. Proteins bound to Protein G were eluted by boiling in Laemmli buffer for 5 min then used to Western blot, as described above.

In vivo permeability assay

Male Sprague-Dawley rats (Charles River Laboratories, Wilmington, MA, USA) were anesthetized with ketamine and xylazine (66.7mg and 6.7mg/kg body weight, intramuscular), and a 32-gauge needle was used to create a hole for an intra-vitreal injection (2.5μl/eye) using a 5-μl Hamilton syringe. Animals received an intra-vitreal injection of either vehicle (PBS, 32% EtOH, 1.3% DMSO), VEGF (50ng), aPKC inhibitor pro-drug (aPKC-I-PD) at 103.8ng or 259.5ng to yield an estimated final vitreous concentration of 10 μM or 25 μM, assuming 30 ul vitreous volume, or atypical PKC inhibitor dichloro substituted (aPKC-I-diCl) at 247.5 ng to yield 25 μM estimated vitreous concentration. Experimental groups received both inhibitor and VEGF simultaneously. The animals recovered for 3 hrs and then were anesthetized again for permeability assay. BRB permeability was assessed by measuring retinal Evan's Blue dye accumulation [32].

Library screen for aPKC inhibitors and *in vitro* high-throughput (HT) kinase assay

The DIVERSet collection of 50,000 compounds from Chembridge (San Diego, CA) was screened for aPKC isoform inhibition using recombinant human PKCζ (100μM) (Enzo Life Sciences Plymouth Meeting, PA), CREBtide (100μM) (Enzo Life Sciences, Plymouth Meeting, PA) as a substrate. The Kinase-Glo luminescence kit from Promega (Madison, WI, USA) was used to measure residual ATP following 3 h incubation. Hits were defined as compounds that inhibited PKCζ activity by at least 50%, and were further characterized in dose-response assays to determine potencies. Further structure-activity relationships (SAR) were performed using the Kinase-Glo luminescence kit with PKCζ (125 ng/ml), ATP (0.1 uM), and CREBtide (25 uM). Specificity profiling was performed by Millipore Corporation using a ^{32}P radiolabeled kinase assay at the K_{mapp} for ATP.

Enzyme kinetic studies

ADP Quest assay (Discover Rx, Fremont, CA, USA) was used to determine inhibitor mechanism of action. Briefly, for ATP competition, compounds were serially diluted and incubated for 1 h at 30°C with 500 ng/ml PKCζ, 100 uM CREBtide, in the presence of a serial dilution of ATP. Substrate competition was performed using similar conditions with a serial dilution of compound and 250 μM ATP, 500 ng/mL PKCζ, and a serial dilution of CREBtide. ADP formation was measured on SpectraMax M5 (Molecular Devices, Sunnyvale, CA, USA) in kinetic mode reading fluorescence at excitation/emission 530/590 every 2.5 min. The signal obtained was converted to rate ([RFU-$RFU_{control}$]/time) and plotted against substrate concentration. $RFU_{control}$ is the signal obtained in the absence of kinase at the respective substrate competition. The data were fitted to the Michaelis-Menten equation using Prism software (Graphpad Software, La Jolla, CA, USA) to obtain K_m values:

$$\text{Rate} = V_{max} * [S] / ([S] + K_m)$$

IC_{50} values were calculated using variable slope Sigmoidal Dose-Response curve. K_i values were derived by plotting the effect of varying substrate concentration on enzyme activity in

the presence of varying concentrations of inhibitor [I]. The data was fitted using global nonlinear regression for non-competitive inhibition with the following equations:

$$V_{maxinh} = V_{max} / (1 + [I] / K_i)$$
$$Rate = V_{maxinh} * [S] / (K_m + [S])$$

Chemical Synthesis

5-Methyl-4-phenyl-2-(substituted-benzoylamino)-thiophene-3-carboxylic acid ethyl ester. Substituted-benzoylamino thiophenes were prepared and verified by ^{1}H-NMR and LC/MS using a modified procedure [33]. 2-Acetylamino-5-methyl-4-phenyl-thiophene-3-carboxylic acid ethyl ester. 40 mg, 34 %; oil; ^{1}H NMR(500 MHz, $CDCl_3$) δ 0.79-0.82 (t, J=7.5 Hz, 3H, CH_3), 2.15 (s, 3H, $=CCH_3$), 2.29 (s, 3H, CH_3), 3.95-4.00 (q, J=7.5 Hz, 2H, OCH_2), 7.15-7.16 (d, J = 5 Hz, 2H, Ar-H), 7.31-7.37 (m, 3H, Ar-H), 11.28 (s, 1H, NH). 2-(2-Chloro-5-nitro-benzoylamino)-5-methyl-4-phenyl-thiophene-3-carboxylic acid ethyl ester. 138 mg(yellow powder), m.p.: 88-90 °C; Sample: ^{1}H NMR(500 MHz, $CDCl_3$) δ 0.80-0.83 (t, J=7.5 Hz, 3H, CH_3), 2.22 (s, 3H, $=CCH_3$), 3.97-4.01 (q, J=7.5 Hz, 2H, OCH_2), 7.19-7.20 (d, J = 5 Hz, 2H, Ar-H), 7.34-7.41 (m, 3H, Ar-H), 7.70-7.72 (d, J=10 Hz, 1H, Ar-H), 8.31-8.33 (d, J=10 Hz, 1H, Ar-H), 8.72 (s, 1H, Ar-H), 12.16 (s, 1H, NH); MS m/z (rel intensity) 444.31 (M^+ , 30), 445.31(15), 446.31(15). 2-Acetylamino-5-methyl-4-phenyl-thiophene-3-carboxylic acid ethyl ester. ^{1}H NMR(500 MHz, $CDCl_3$) δ 2.14 (s, 3H, $=CCH_3$), 2.31 (s, 3H, CH_3), 7.38-7.40 (m, 2H, Ar-H), 7.31-7.37 (m, 3H, Ar-H), 11.13 (s, 1H, NH). MS m/z (rel intensity) 275.048 (M^+, 15), 276.058(30). 2-amino-4-(chlorophenyl) thiophene-3-3-carboxylate. MS m/z (rel intensity) 253.38 (M^+, 30), 254.38(15). 2-Acetylamino-4-(4-chloro-phenyl)-thiophene-3-carboxylic acid ethyl ester MS m/z (rel intensity) 323.48 (M^+ , 35), 324.48(20). 2-(2-Chloro-5-nitro-benzoylamino)-4-(4-chloro-phenyl)-thiophene-3-carboxylic acid ethyl ester MS m/z (rel intensity) 464.38 (M^+ , 45), 465.38(10). 2-(2-Chloro-5-fluoro-benzoylamino)-4-(4-chloro-phenyl)-thiophene-3-carboxylic acid ethyl ester MS m/z (rel intensity) 437.46 (M^+ , 35), 438.46(10).

Immuno-cytochemistry and confocal microscopy

Cells were grown to confluence on plastic coverslips then serum starved with Endogro (ZO-1), without Endogro (Occludin) for 24 h. The ommitance of endogro when staining for occludin is required to maximize occludin staining at the periphery of endothelial cells, which has been demonstrated previously [22]. Cells were treated as indicated then fixed with 1% paraformaldehyde for 10 min at room temperature followed by permeabilization with 0.2% Triton X-100 for ZO-1 or pre-extracted with high sucrose buffer fixed with ethanol on ice for 30 min for occludin [34]. Following blocking with 10% goat serum (ZO-1) or 10% BSA (occludin) in 0.1% Triton X-100, cells were stained with a rat monoclonal ZO-1 antibody or polyclonal rabbit occludin antibody and fluorescently imaged as previously described [23]. Occludin localization in retinal vessels was assessed by immunohistochemistry in whole retinas, as described previously [17] and displayed as collapsed serial images. Imaging was accomplished using a Leica confocal microscope and imaging software (TCS SP2 AOBS; Leica; Wetzlar, Germany).

Statistical analysis of data

All studies were performed in duplicate or triplicate and presented either as a compilation of multiple independent experiments or representative of multiple experiments. Unless otherwise stated, statistical analysis was carried out using Prism software from Graphpad using one-way analysis of variance (ANOVA) with the Neuman-Keuls post-hoc analysis or Student's t-test. A p value of less than 0.05 was considered statistically significant. Number of sample size is indicated in figure legends.

RESULTS

VEGF treatment activates aPKC isoforms in rodent retina and primary endothelial cells

In order to investigate if aPKC isoforms contribute to VEGF-induced retinal permeability *in vivo,* Sprague-Dawley rats were intra-vitreally injected with VEGF and retinas were excised and probed for autophosphorylation of PKCζ/ι at Thr560/Thr555. VEGF induced aPKC autophosphorylation within 15 minutes and was maximal at 30 min with an approximately 3 fold increase relative to sham injection (Fig. 1A). The PI3K-dependent priming phosphorylation site, Thr410/Thr412, was probed using a phospho-specific antibody to pThr410/412 PKCζ/ι [28]. VEGF increased phosphorylation of this residue within 15 min (Fig. 1B) and returned to basal following longer time points. Further mechanistic studies were carried out using primary bovine retinal endothelial cells (BREC) to further define the contribution of aPKC signaling to VEGF-induced endothelial permeability. First, conservation of the VEGF-induced activation for aPKC isoforms was determined. BREC were treated with VEGF for 15 minutes followed by Western blotting utilizing phospho-specific antibodies. VEGF activates aPKC isoforms as measured by a 2-fold increase in phosphorylation at Thr410/Thr412 with a more modest but significant increase at Thr560/Thr555 (Fig. 1C). Robust VEGF intra-cellular signaling was verified in these cells demonstrated by a significant increase in phosphorylated ERK1/2 (Fig. 1C).

aPKC isoforms contribute to VEGF-induced retinal endothelial permeability

To determine the role of aPKC isoforms in VEGF-induced permeability, genetic manipulation of aPKCζ expression was performed. Expression plasmid for FLAG-tagged wild-type aPKCζ was transfected into BREC (Fig. 2A), and the cells were grown to confluence on 0.4 μm Transwell filters. VEGF treatment of control cells increased the permeability of the monolayer to 70 kDa RITC-Dextran 1.5-2.0-fold, an effect that was significantly potentiated with the overexpression of wild-type aPKCζ (Fig. 2A). Furthermore, BREC were transduced with recombinant adenoviruses containing a wild-type PKCζ (AdWTaPKCζ), kinase-dead PKCζ mutant (AdKDaPKCζ), and a constitutively active mutant of PKCζ (AdCAaPKCζ) (Fig. 2B). Overexpression of AdKDaPKCζ completely prevented the VEGF-induced permeability to 70kDa RITC-Dextran in primary endothelial cells (Fig. 2C). Additionally, AdCAaPKCζ alone was sufficient to significantly augment basal permeability in BREC compared to AdGFP or AdWTaPKCζ transduced cells demonstrating that overexpression of an active aPKC isoform is sufficient to increase permeability in retinal endothelial cells without stimulus (Fig. 2D).

PKCι mediates VEGF-induced permeability in primary retinal endothelial cells

To investigate which aPKC isoforms are specifically expressed in our primary retinal endothelial model and to avoid the complications associated with differences in primer efficiency, homologous primers were designed to amplify PKC zeta and iota that contain unique restriction sites within the amplicon to differentiate between the two aPKC isoforms. Following cDNA library generation, these homologous aPKC primers were used to amplify aPKCζ/ι. Restriction digestions were performed to identify which aPKC isoforms were expressed and to determine the relative stoichiometric ratio of expression in BREC. Digestion with Pst1 (PKCι specific) completely digested the 470 bp amplicon of aPKC and Stu1 (PKCζ specific) failed to digest this amplicon (Fig. 3A) suggesting PKCι is the primary aPKC expressed in BREC. Both restriction enzymes were shown to be active against lambda DNA (data not shown). Multiple siRNAs were designed and generated to target the aPKC isoforms in BREC. Multiple PKCζ specific siRNAs failed to knockdown aPKC protein content in BREC further supporting that PKCι is the primary isoform expressed (Supplemental Fig. 1A). Importantly, three siRNA duplexes targeting PKCι significantly decreased aPKC protein content within 72 h (Fig. 3B). PKCι Constructs A, C and D resulted

in a robust knockdown (~60-80%), in aPKC content (Fig. 3B). BREC were transfected with PKCι Constructs A, C, and D and VEGF-induced permeability was assessed. All three constructs prevented the VEGF-induced increase in retinal endothelial permeability (Fig. 3C).

Peptide inhibition of aPKC isoforms prevents VEGF-induced retinal endothelial permeability

To determine if aPKC kinase activity is essential for the VEGF-induced increase in endothelial permeability, a pseudosubstrate (PS) peptide inhibitor of aPKC isoforms (aPKC-PS) was used to block the kinase activity of the enzyme. This inhibitor is a myristoylated peptide corresponding to the auto-inhibitory pseudosubstrate domain of aPKC isoforms [35]. BREC were grown to confluence on Transwell filters and cells were treated with the indicated dose of aPKC-PS for 30 min prior to VEGF treatment. Permeability to 70kDa RITC-Dextran was measured over 4 h, starting 30 min after addition of VEGF. The aPKC-PS inhibited VEGF-induced permeability in a dose-responsive manner (Fig. 4A). Repeat experiment using 50 nM aPKC inhibitor demonstrated significant reduction of the VEGF-induced BREC permeability (Fig. 4B).

The identification and characterization of small molecule phenyl-thiophene inhibitors of aPKC isoforms

Although aPKC-PS is a potent inhibitor of aPKC isoforms, it is impractical to use as a drug because of poor bioavailability and pharmacodynamic profile characteristics of PKC peptide inhibitors. Therefore, in order to identify novel, small molecule inhibitors of atypical PKC for potential therapeutic intervention, a 50,000 member chemical library from Chembridge was screened for compounds that inhibit recombinant PKCζ kinase activity in an *in vitro* assay. Initially, a library screen of compounds was performed at a concentration of 100 μM using purified recombinant PKCζ and 25 μM CREBtide as a PKC substrate. The Kinase-Glo luminescence kit was used to measure residual ATP concentration following 3 h room temperature incubation. Hits were defined as compounds that inhibited rPKCζ activity by at least 50%, and these were further characterized in dose-response assays to determine their potencies and specificities. A total of 14 compounds with IC_{50} values of 100 μM or less were identified representing a 0.03% hit rate, and a group of compounds with molecular weights below 500 that showed structural similarity were identified. A number of the compounds contained a phenyl-thiophene core structure; therefore, additional screening was focused on phenyl-thiophene derivatives and IC_{50} values were determined in order to elucidate a pharmacophore (Fig. 5A & 5B). From these studies three drugs were identified for additional studies, a pro-drug (PD) for its favorable bioavailability profile for *in vivo* administration (aPKC-I-PD) and two stable derivatives with the lowest IC_{50} from this class of compounds, one with a dichloro substituted phenyl ring (aPKC-I-diCl), and a similar molecule with a dimethoxy substituted phenyl-thiophene (aPKC-I-diMeO) (Fig. 5B). From the list of compounds in Fig. 5A an initial structure-activity relationship was performed to identify the core pharmacophore required for *in vitro* activity. From this analysis it was deduced that a 1° amine functionality at the R2 position is required for activity (Fig. 5B). aPKC-I-PD possesses an amide bond at this position that likely is susceptible to protease cleavage within a cellular environment. The loss of the hydroxyiminoethyl at R1, coupled with the amide bond cleavage was determined as necessary for an active compound *in vitro.*

One of the most potent PKCζ inhibitors, aPKC-I-diMeO, was selected for mechanism of action studies due to its improved solubility in aqueous environments. A competition assay was performed to determine the mechanism of action for this class of compounds. By measuring ADP formation under increasing ATP concentrations at various doses of inhibitor, it was determined that aPKC-I-diMeO significantly altered V_{max} without affecting

K_m with a K_i 7 ± 5 μM (Fig. 6A). Furthermore, a similar competition assay was performed against CREBtide, a short peptide PKC substrate, and the peptide substrate also failed to compete the aPKC-I-diMeO inhibitor and restore V_{max} (Fig. 6B). Thus, 2-amino-4-phenyl-thiophenes are non-competitive inhibitors of PKCζ.

aPKC-I-diCl and aPKC-I-diMeO were screened against other PKC isoforms to determine class specificity using a radio-labeled kinase assay at the $K_{m\ app}$ for ATP. aPKC-I-diCl is 5-10 fold more specific towards the atypical PKC isoforms compared to the classical PKCs (α, β) and over 10-20 fold more specific compared to the novel class (δ, ε) (Fig. 6C). aPKC-I-diMeO improves on specificity against the classical PKC isoforms having a 25-50 fold lower IC_{50} compared to α, β while also maintaining a 25 fold lower IC_{50} towards the novel class (δ, ε) (Fig. 6C). These compounds do not exhibit specificity within the atypical PKC class, which share significant homology with similar IC_{50} values for PKCι and PKCζ. To determine if aPKC-I-diMeO possesses significant inhibitor activity towards other kinases, 20 AGC super-family kinases sharing the most similar sequence homology to PKCs, were screened at 100 uM, ~20 fold the K_i for aPKC isoforms. aPKC-I-diMeO has limited inhibitory activity to these other kinases with only a modest reduction in two other PKC isoforms tested (Fig. 6D). Additionally, the aPKC–I-diMeO does not inhibit cPKC activity in cell culture. Erk phosphorylation, which is downstream of cPKC in endothelial cells, was unaffected by aPKC-I-diMeO treatment (Fig. 6E). Furthermore, AKT a downstream mediator of PI3K signaling in endothelial cells, was also unaffected by aPKC-I-diMeO treatment (Fig. 6E) Finally, aPKC-I-diMeO inhibits an active kinase fragment devoid of regulatory domains (amino acids 211-592) of rPKCζ as effectively as it inhibits full length rPKCζ demonstrating it acts within this region of the kinase (data not shown). Collectively, these studies demonstrate that phenyl-thiophene derivatives are potent inhibitors of aPKC isoforms with high specificity and a pharmacophore has been delineated.

Phenyl-thiophenes prevent VEGF-induced vascular endothelial permeability

The effectiveness of these phenyl-thiophenes in preventing VEGF-induced endothelial permeability was determined. Primary BREC were grown to confluence on 0.4 μm Transwell filters as above and pretreated with 10 or 25 μM aPKC-I-PD for 30 min prior to treatment with 50 ng/ml VEGF. The permeability of the monolayer to 70 kDa RITC-Dextran was measured and the Po determined. At both doses, the PKCζI-PD was able to completely block the VEGF-induced increase in endothelial permeability with micromolar potency (Fig. 7A). Further, aPKC-I-diCl blocked VEGF-induced permeability in BREC at approximately 100 fold lower concentration (Fig. 7B). The dimethoxy substituted aPKC-I-diMeO displayed similar potency as the aPKC-I-diCl in its ability to effectively block VEGF-induced endothelial permeability (Fig. 7C). Dose response efficacy curves were determined and aPKC-I-diMeO failed to significantly prevent VEGF-induced permeability below 10 nM (Supplemental Fig. 2A) while aPKC-I-PD failed to block VEGF-induced permeability in the nanomolar range (Supplemental Fig. 2B). Measures of BREC viability at 24 and 48h revealed no evidence of cell death after treatment with aPKC-I-PD at up to 30μM, aPKC-I-diCl at up to 300 nM or aPKC-I-diMeO at up to 300 nM (Supplemental Fig. 3A & 3B).

To further examine the role of aPKC isoforms on steady state barrier regulation, a dose-response curve with the phenyl-thiophenes was performed. BREC were plated on Transwell filters as above and treated with aPKC-I-PD at doses ranging from 10 to 0.1 μM for 30 min prior to the addition of the fluorescent tracer. The compound significantly decreased the permeability of the BREC monolayer at a dose as low as 1 μM (Supplemental Fig. 4A). This basal effect of reducing permeability also can be observed in human retinal endothelial primary cells (HREC) monolayers with the aPKC-I-diCl molecule, (Supplemental Fig. 4B).

These data demonstrate aPKC isoforms play an important role in barrier homeostasis in endothelial monolayers.

aPKC inhibition prevents disorganization of tight junctions proteins following VEGF treatment

VEGF treatment of retinal endothelial cells and retinal vasculature alters the tight junction complex and induces internalization of tight junction proteins occludin and ZO-1 [16, 18, 36]. The ability of the phenyl-thiophene derivatives to prevent the VEGF-induced reduction in tight junction border staining was examined. BREC were grown to confluence on coverslips and pretreated with 10 μM aPKC-I-PD or 100 nM aPKC-I-diCl for 30 min prior to treatment with 50 ng/ml VEGF for 60 min. Cells were fixed and stained with antibodies for ZO-1 (Fig. 8A) or occludin (Fig. 8B) and were visualized by confocal miscroscopy. VEGF decreased the border staining and continuity of ZO-1 and occludin labeling at the cell border as expected. Pretreatment of cells with both aPKC inhibitors blocked the VEGF-induced redistribution of tight junction proteins and preserved continuous border staining suggesting that inhibition of aPKC acts to preserve barrier properties by preventing a net movement of tight junction proteins from the plasma membrane into the cytoplasm and preventing the formation of tight junction breaks.

aPKC-Is block the VEGF induction of retinal vascular permeability *in vivo*

To determine if aPKC-Is block retinal vascular permeability *in vivo*, we tested the ability of aPKC-I-PD and aPKC-I-diCl to block the VEGF-induced extravasation of Evan's blue dye in the retina. Sprague-Dawley rats (150-175 g) received 5 μl intra-vitreal injections of either vehicle, or a final estimated vitreous concentration of 25 μM PKCζI-PD (Fig. 9A) or PKCζI-diCl (Fig. 9B), 50 ng VEGF, or aPKC-I plus VEGF as indicated. Treatment with VEGF caused an approximate 60-70% increase in accumulation of Evan's blue in the retina (Fig. 9A and 9B). Administration of 25 μM of either aPKC-I prevented the VEGF-induced increase in retinal Evan's blue dye accumulation (Fig. 9A and 9B). Dose dependence was observed as administration of 10 μM aPKC-I-PD partially blocked blood-retinal barrier breakdown in response to VEGF (Supplemental Fig. 5).

To determine the effects of aPKC isoform inhibition on the retinal vasculature tight junction complex, retinal flat mounts were prepared and immuno-labeled with occludin following the intravitreal injection of VEGF and/or aPKC-I-diCl. In vehicle-injected eyes, occludin border staining was intense and continuous; however, upon VEGF treatment, the immuno-reactivity was decreased and a discontinuous border-staining pattern was observed (Fig. 9C). Upon aPKC-I-diCl co-injection, occludin border staining was preserved and there were no longer instances of a discontinuous occludin staining (Fig. 9C). Of note, functional electroretinograms (ERGs) were performed 5 hrs following vehicle or aPKC-I-diCl (25 μM) injections to determine if the small molecule aPKC inhibitors affected retinal function. There was no statistical difference in either B or A-wave amplitude in either light or dark-adapted Long Evan's rats (Supplemental Fig. 6A & 6B). Moreover, there was no evidence of morphological defects or retinal cell death following aPKC inhibitor injections (Supplemental Fig. 7). These results, combined with the cell culture studies, demonstrate that inhibiting aPKC in retinal endothelial cells prevents VEGF-induced breaks in the tight junction complex and subsequent retinal vascular permeability without causing measurable retinal toxicity or functional defects.

DISCUSSION

Macular edema contributes to the pathophysiology of a number of retinal diseases including diabetic retinopathy, ischemic retinopathies and uveitis among others [37]. It is now well

established that VEGF, a potent vascular permeabilizing agent, contributes to retinal macular edema particularly in diabetic and ischemic retinopathies. Previous research has focused on the contribution of classical PKC isoforms downstream of VEGF signaling. Hyperglycemia and advanced glycation end products (AGEs) activate cPKC contributing to VEGF expression or release. Downstream of VEGF, cPKC isoforms are implicated in numerous diabetic vascular complications [13]. In particular, PKCβ contributes to diabetes induced-endothelial proliferation and permeability and oral administration of a specific PKCβ inhibitor, ruboxistaurin, prevents these pathologic outcomes [14, 15]. Recent clinical trials suggest ruboxistaurin delays sustained moderate visual loss in diabetic retinopathy [38]. Unfortunately, these inhibitors are only partially effective at blocking VEGF-induced permeability in retinal endothelial cells [19] and have not yet achieved FDA approval as therapeutics. In addition to VEGF, pro-inflammatory cytokines such as TNFα also contribute to diabetic retinopathy disease pathogenesis [9] and compounds that prevent both the angiogenic and inflammatory components of retinopathy may prove most effective [39]. Thus, the discovery and generation of novel therapies that prevent or improve these vasculopathies are warranted.

Here we report a novel function for aPKC isoforms in regulation of tight junction breaks and vascular permeability in response to VEGF. Further, we identify a novel class of aPKC small molecule inhibitors that prevent VEGF-induced BRB breakdown and describe a pharmacophore for these inhibitors. The novel compounds act as non-competitive inhibitors in respect to both ATP and substrate binding with high specificity for the aPKC isoforms. Further, no evidence of endothelial cell toxicity or functional retinal defects were observed with inhibitor treatment. Importantly, the inhibitors were effective at completely blocking VEGF-induced 70kDa dextran permeability in cell culture and albumin permeability in the retina *in vivo*. Published data from our laboratory demonstrate a role for aPKC in TNFα induced permeability, which was blocked by the aPKC-I-PD [23]. Together, these data demonstrate a novel aPKC inhibitor class that effectively blocks both growth factor and inflammatory cytokine-induced vascular permeability.

Recent data implicates aPKC isoforms in endothelial barrier breakdown and disassembly following a number of pathological insults. Signaling through aPKC is required for TNFα-induced barrier disruption [23], thrombin-induced endothelial permeability [40, 41], and ischemia-induced blood-brain barrier dysfunction [42]. Data presented herein demonstrates a necessity for aPKC signaling in VEGF-induced barrier destabilization and vascular permeability. Alternatively, previous data suggests aPKC isoforms are important for barrier assembly and junctional formation evident from the PKCλ knockout [43]. How aPKC promotes both assembly and disassembly of the junctional complex is not completely understood and likely depends on location, specific signaling pathways, and the degree of junctional assembly. A similar role in both pro- and anti-barrier properties exists for the Rho family of GTPases [44, 45]. Indeed RhoA promotes barrier destabilization when activated by VEGF [46] or downstream of GEF-H1 [47] but spatially restricted activation of RhoA by p114RhoGEF promotes junction formation [48]. The specific downstream mediators and direct substrates of aPKC signaling and their role in barrier function in retinal endothelial cells will be the basis of future investigations. Importantly, the requirement for aPKC isoforms in VEGF-induced endothelial permeability is shown here through the use of multiple genetic and pharmacological manipulations.

The high-degree of sequence homology of the aPKC isoforms makes it difficult to determine which isoforms contribute to a specific disease phenotype without the use of genetic loss-of-function experiments. Although data from systemic knockout animals suggests distinct phenotypes, there is emerging evidence that aPKC isoforms may play redundant roles. For instance, aPKC isoforms share a redundant mechanism in insulin-simulated-glucose uptake

in adipocyte and muscle cells [49, 50]. Our data indicates the predominate isoform expressed in BREC is PKCι where we demonstrate using multiple siRNA oligonucleotide duplexes that knockdown of PKCι is sufficient to prevent VEGF-induced permeability. Furthermore, our novel small molecule inhibitors inhibit both aPKC isoforms with no degree of specificity. The degree of isoform specific contribution to retinal vascular permeability in animals will be elucidated in future studies. Importantly, we demonstrated aPKC isoforms are novel downstream targets of VEGF and novel small molecule inhibitors of this class of kinases are effective at preventing the deleterious effect of VEGF-induced permeability.

While the biology and emerging significance of the aPKC isoforms has become apparent, the lack of readily available potent and specific small molecule inhibitors has hindered both preclinical and clinical studies on this class of kinase. Studies have identified limited small molecule inhibitors of aPKC; however, some of these compounds lack specificity and potency [51-56]. Recent evidence using a class of aPKC inhibitors has been shown in some models of type II diabetes to be able to correct the metabolic abnormalities of the disease [57]. In this study, aPKC was demonstrated as necessary for VEGF induced hyper-permeability and a non-competitive, highly specific aPKC inhibitor pharmacophore was identified. The phenyl-thiophene inhibitor demonstrated low micromolar K_i with similar potency for aPKC isoforms. These compounds prevent both VEGF and inflammatory cytokine-induced endothelial permeability and may be developed as novel therapies for the treatment of macular edema resulting from various ocular diseases and may be useful in treatment of BBB dysfunction during inflammation, cerebral injury and brain tumors.

Supplementary Material

Refer to Web version on PubMed Central for supplementary material.

Acknowledgments

We greatly appreciate the gifts of pCMV-FLAG-aPKCζ from Dr. Alex Toker (Harvard University) and AdWTaPKCζ, AdKDaPKCζ, and AdCAaPKCζ from Dr. Adolfo Garcia-Ocaña (University of Pittsburgh). We would like to thank all members of the Penn State Retina Research Group for their insights and thoughtful suggestions and in particular Ellen B. Wolpert (Penn State University) and Edward Felinski (Penn State University) for their technical support and expertise. We would also like to thank Dr. Lynn Maines (Apogee, Inc.) and all of Apogee, Inc. for their insights and technical support.

FUNDING

This research was supported by the National Institutes of Health Grants EY012021 (to D.A.A.) and core grants EY07003 and DK020572, the JDRF Research Foundation (to D.A.A.), the Jules and Doris Stein Professorship from Research to Prevent Blindness (to D.A.A.) and the Fight for Sight Research Foundation (to P.M.T). No potential conflicts of interest relevant to this article were reported.

Abbreviations used are

TJ	tight junction
BRB	blood-retinal barrier
VEGF	vascular endothelial growth factor
BBB	blood-brain barrier
ZO-1	zonula occludens-1
RECs	retinal endothelial cells
RITC	rhodamine B isothiocyanate

PKC	Protein Kinase C
aPKC	atypical PKC
AdWTaPKCζ	adenovirus containing wild-type PKC zeta transgene
AdCAaPKCζ	adenovirus containing c-src myristoylation sequence inducing membrane localization and activation
AdKDaPKCζ	adenovirus containing PKC zeta transgene with a kinase dead mutation
pCMV-FLAG-aPKCζWT	plasmid construct containing wild type PKC zeta
and aPKC-I	a small molecule aPKC inhibitor
aPKC-PS	peptide inhibitor of aPKC mimicking pseudosubstrate domain
PAR	partition defective homologue
Glut4	Glucose Transport 4
IL-1	Interleukin-1
TNFα	Tumor Necrosis Factor α

REFERENCES

1. Antonetti DA, Barber AJ, Bronson SK, Freeman WM, Gardner TW, Jefferson LS, Kester M, Kimball SR, Krady JK, LaNoue KF, Norbury CC, Quinn PG, Sandirasegarane L, Simpson IA. Diabetic retinopathy: seeing beyond glucose-induced microvascular disease. Diabetes. 2006; 55:2401–2411. [PubMed: 16936187]
2. Gardner TW, Larsen M, Girach A, Zhi X. Diabetic macular oedema and visual loss: relationship to location, severity and duration. Acta Ophthalmologica. 2009; 87:709–713. [PubMed: 19817721]
3. Sander B, Thornit DN, Colmorn L, Strom C, Girach A, Hubbard LD, Lund-Andersen H, Larsen M. Progression of diabetic macular edema: correlation with blood retinal barrier permeability, retinal thickness, and retinal vessel diameter. Investigative ophthalmology & visual science. 2007; 48:3983–3987. [PubMed: 17724176]
4. Antonetti DA, Klein R, Gardner TW. Diabetic retinopathy. N. Eng. J. Med. 2012; 366:1227–1239.
5. Penn JS, Madan A, Caldwell RB, Bartoli M, Caldwell RW, Hartnett ME. Vascular endothelial growth factor in eye disease. Prog. Retin. Eye. Res. 2008; 27:331–371. [PubMed: 18653375]
6. Aiello LP, Avery RL, Arrigg PG, Keyt BA, Jampel HD, Shah ST, Pasquale LR, Thieme H, Iwamoto MA, Park JE, et al. Vascular endothelial growth factor in ocular fluid of patients with diabetic retinopathy and other retinal disorders. N. Eng. J. Med. 1994; 331:1480–1487.
7. Aiello LP. Vascular endothelial growth factor and the eye: biochemical mechanisms of action and implications for novel therapies. Ophthalmic. Res. 1997; 29:354–362. [PubMed: 9323726]
8. Demircan N, Safran BG, Soylu M, Ozcan AA, Sizmaz S. Determination of vitreous interleukin-1 (IL-1) and tumour necrosis factor (TNF) levels in proliferative diabetic retinopathy. Eye (Lond). 2006; 20:1366–1369. [PubMed: 16284605]
9. Joussen AM, Poulaki V, Mitsiades N, Kirchhof B, Koizumi K, Dohmen S, Adamis AP. Nonsteroidal anti-inflammatory drugs prevent early diabetic retinopathy via TNF-alpha suppression. FASEB J. 2002; 16:438–440. [PubMed: 11821258]
10. Salam A, Mathew R, Sivaprasad S. Treatment of proliferative diabetic retinopathy with anti-VEGF agents. Acta. Ophthalmol. 2011
11. Elman MJ, Bressler NM, Qin H, Beck RW, Ferris FL 3rd, Friedman SM, Glassman AR, Scott IU, Stockdale CR, Sun JK. Expanded 2-Year Follow-up of Ranibizumab Plus Prompt or Deferred Laser or Triamcinolone Plus Prompt Laser for Diabetic Macular Edema. Ophthalmology. 2011; 118:609–614. [PubMed: 21459214]

12. Elman MJ, Aiello LP, Beck RW, Bressler NM, Bressler SB, Edwards AR, Ferris FL 3rd, Friedman SM, Glassman AR, Miller KM, Scott IU, Stockdale CR, Sun JK. Randomized trial evaluating ranibizumab plus prompt or deferred laser or triamcinolone plus prompt laser for diabetic macular edema. Ophthalmology. 2010; 117:1064–1077. e1035. [PubMed: 20427088]
13. Das Evcimen N, King GL. The role of protein kinase C activation and the vascular complications of diabetes. Pharmacol. Res. 2007; 55:498–510. [PubMed: 17574431]
14. Ishii H, Jirousek MR, Koya D, Takagi C, Xia P, Clermont A, Bursell SE, Kern TS, Ballas LM, Heath WF, Stramm LE, Feener EP, King GL. Amelioration of vascular dysfunctions in diabetic rats by an oral PKC beta inhibitor. Science. 1996; 272:728–731. [PubMed: 8614835]
15. Aiello LP, Bursell SE, Clermont A, Duh E, Ishii H, Takagi C, Mori F, Ciulla TA, Ways K, Jirousek M, Smith LE, King GL. Vascular endothelial growth factor-induced retinal permeability is mediated by protein kinase C in vivo and suppressed by an orally effective beta-isoform-selective inhibitor. Diabetes. 1997; 46:1473–1480. [PubMed: 9287049]
16. Antonetti DA, Barber AJ, Khin S, Lieth E, Tarbell JM, Gardner TW. Vascular permeability in experimental diabetes is associated with reduced endothelial occludin content: vascular endothelial growth factor decreases occludin in retinal endothelial cells. Penn State Retina Research Group. Diabetes. 1998; 47:1953–1959. [PubMed: 9836530]
17. Barber AJ, Antonetti DA, Gardner TW. Altered expression of retinal occludin and glial fibrillary acidic protein in experimental diabetes. The Penn State Retina Research Group. Invest. Ophthalmol. Vis. Sci. 2000; 41:3561–3568. [PubMed: 11006253]
18. Antonetti DA, Barber AJ, Hollinger LA, Wolpert EB, Gardner TW. Vascular endothelial growth factor induces rapid phosphorylation of tight junction proteins occludin and zonula occluden 1. A potential mechanism for vascular permeability in diabetic retinopathy and tumors. J. Biol. Chem. 1999; 274:23463–23467. [PubMed: 10438525]
19. Harhaj NS, Felinski EA, Wolpert EB, Sundstrom JM, Gardner TW, Antonetti DA. VEGF activation of protein kinase C stimulates occludin phosphorylation and contributes to endothelial permeability. Invest. Ophthalmol. Vis. Sci. 2006; 47:5106–5115. [PubMed: 17065532]
20. Sundstrom JM, Tash BR, Murakami T, Flanagan JM, Bewley MC, Stanley BA, Gonsar KB, Antonetti DA. Identification and analysis of occludin phosphosites: a combined mass spectrometry and bioinformatics approach. J. Proteome Res. 2009; 8:808–817. [PubMed: 19125584]
21. Murakami T, Frey T, Lin C, Antonetti DA. Protein Kinase Cbeta Phosphorylates Occludin Regulating Tight Junction Trafficking in Vascular Endothelial Growth Factor-Induced Permeability In Vivo. Diabetes. 2012 epub ahead of print.
22. Murakami T, Felinski EA, Antonetti DA. Occludin phosphorylation and ubiquitination regulate tight junction trafficking and vascular endothelial growth factor-induced permeability. J. Biol. Chem. 2009; 284:21036–21046. [PubMed: 19478092]
23. Aveleira CA, Lin CM, Abcouwer SF, Ambrosio AF, Antonetti DA. TNF-alpha signals through PKCzeta/NF-kappaB to alter the tight junction complex and increase retinal endothelial cell permeability. Diabetes. 2010; 59:2872–2882. [PubMed: 20693346]
24. Abu el Asrar AM, Maimone D, Morse PH, Gregory S, Reder AT. Cytokines in the vitreous of patients with proliferative diabetic retinopathy. Am. J. Ophthalmol. 1992; 114:731–736. [PubMed: 1463043]
25. Sharma SM, Nestel AR, Lee RW, Dick AD. Clinical review: Anti-TNFalpha therapies in uveitis: perspective on 5 years of clinical experience. Ocular immunology and inflammation. 2009; 17:403–414. [PubMed: 20001261]
26. Hirai T, Chida K. Protein kinase Czeta (PKCzeta): activation mechanisms and cellular functions. Biochem. J. 2003; 133:1–7.
27. Steinberg SF. Structural basis of protein kinase C isoform function. Physiol. Rev. 2008; 88:1341–1378. [PubMed: 18923184]
28. Chou MM, Hou W, Johnson J, Graham LK, Lee MH, Chen CS, Newton AC, Schaffhausen BS, Toker A. Regulation of protein kinase C zeta by PI 3-kinase and PDK-1. Curr. Biol. 1998; 8:1069–1077. [PubMed: 9768361]
29. Antonetti DA, Wolpert EB. Isolation and characterization of retinal endothelial cells. Meth. Mol. Med. 2003; 89:365–374.

30. DeMaio L, Antonetti DA, Scaduto RC Jr. Gardner TW, Tarbell JM. VEGF increases paracellular transport without altering the solvent-drag reflection coefficient. Microvasc. Res. 2004; 68:295–302. [PubMed: 15501249]

31. Phillips BE, Cancel L, Tarbell JM, Antonetti DA. Occludin independently regulates permeability under hydrostatic pressure and cell division in retinal pigment epithelial cells. Invest. Ophthalmol. Vis. Sci. 2008; 49:2568–2576. [PubMed: 18263810]

32. Xu Q, Qaum T, Adamis AP. Sensitive blood-retinal barrier breakdown quantitation using Evans blue. Invest. Ophthalmol. Vis. Sci. 2001; 42:789–794. [PubMed: 11222542]

33. Rannard SP, Davis NJ. The selective reaction of primary amines with carbonyl imidazole containing compounds: selective amide and carbamate synthesis. Organic Letters. 2000; 2:2117–2120. [PubMed: 10891244]

34. Balda MS, Whitney JA, Flores C, Gonzalez S, Cereijido M, Matter K. Functional dissociation of paracellular permeability and transepithelial electrical resistance and disruption of the apical-basolateral intramembrane diffusion barrier by expression of a mutant tight junction membrane protein. J. Cell Biology. 1996; 134:1031–1049.

35. Zhou G, Seibenhener ML, Wooten MW. Nucleolin is a protein kinase C-zeta substrate. Connection between cell surface signaling and nucleus in PC12 cells. J. Biol. Chem. 1997; 272:31130–31137. [PubMed: 9388266]

36. Barber AJ, Antonetti DA. Mapping the blood vessels with paracellular permeability in the retinas of diabetic rats. Invest. Ophthalmol. Vis. Sci. 2003; 44:5410–5416. [PubMed: 14638745]

37. Johnson MW. Etiology and treatment of macular edema. Am J Ophthalmol. 2009; 147:11–21. e11. [PubMed: 18789796]

38. Sheetz MJ, Aiello LP, Shahri N, Davis MD, Kles KA, Danis RP. Effect Of Ruboxistaurin (RBX) On Visual Acuity Decline Over a 6-Year Period With Cessation And Reinstitution Of Therapy: Results of an Open-Label Extension of the Protein Kinase C Diabetic Retinopathy Study 2 (PKC-DRS2). Retina. 2011

39. Jung K, Lee D, Lim HS, Lee SI, Kim YJ, Lee GM, Kim SC, Koh GY. Double Anti-angiogenic and Anti-inflammatory Protein Valpha Targeting VEGF-A and TNF-{alpha} in Retinopathy and Psoriasis. J. Biol. Chem. 2011; 286:14410–14418. [PubMed: 21345791]

40. Minshall RD, Vandenbroucke EE, Holinstat M, Place AT, Tiruppathi C, Vogel SM, van Nieuw Amerongen GP, Mehta D, Malik AB. Role of protein kinase Czeta in thrombin-induced RhoA activation and inter-endothelial gap formation of human dermal microvessel endothelial cell monolayers. Microvasc. Res. 2010; 80:240–249. [PubMed: 20417648]

41. Li X, Hahn CN, Parsons M, Drew J, Vadas MA, Gamble JR. Role of protein kinase Czeta in thrombin-induced endothelial permeability changes: inhibition by angiopoietin-1. Blood. 2004; 104:1716–1724. [PubMed: 15172966]

42. Willis CL, Meske DS, Davis TP. Protein kinase C activation modulates reversible increase in cortical blood-brain barrier permeability and tight junction protein expression during hypoxia and posthypoxic reoxygenation. J. Cereb. Blood Flow Metab. 2010; 30:1847–1859. [PubMed: 20700133]

43. Macara IG. Parsing the polarity code. Nat Rev Mol Cell Biol. 2004; 5:220–231. [PubMed: 14991002]

44. Spindler V, Schlegel N, Waschke J. Role of GTPases in control of microvascular permeability. Cardiovasc. Res. 2010; 87:243–253. [PubMed: 20299335]

45. Beckers CM, van Hinsbergh VW, van Nieuw Amerongen GP. Driving Rho GTPase activity in endothelial cells regulates barrier integrity. Thromb. Haemost. 2010; 103:40–55. [PubMed: 20062930]

46. Bryan BA, Dennstedt E, Mitchell DC, Walshe TE, Noma K, Loureiro R, Saint-Geniez M, Campaigniac JP, Liao JK, D'Amore PA. RhoA/ROCK signaling is essential for multiple aspects of VEGF-mediated angiogenesis. FASEB J. 2010; 24:3186–3195. [PubMed: 20400538]

47. Samarin SN, Ivanov AI, Flatau G, Parkos CA, Nusrat A. Rho/Rho-associated kinase-II signaling mediates disassembly of epithelial apical junctions. Mol. Bio. Cell. 2007; 18:3429–3439. [PubMed: 17596509]

48. Terry SJ, Zihni C, Elbediwy A, Vitiello E, Leefa Chong San IV, Balda MS, Matter K. Spatially restricted activation of RhoA signalling at epithelial junctions by p114RhoGEF drives junction formation and morphogenesis. Nature Cell Bio. 2011; 13:159–166. [PubMed: 21258369]

49. Sajan MP, Rivas J, Li P, Standaert ML, Farese RV. Repletion of atypical protein kinase C following RNA interference-mediated depletion restores insulin-stimulated glucose transport. The J. Bio. Chem. 2006; 281:17466–17473.

50. Farese RV, Sajan MP. Metabolic functions of atypical protein kinase C: “good” and “bad” as defined by nutritional status. Am. J. Physiol. Endocrinol. Metab. 2010; 298:E385–394. [PubMed: 19996389]

51. Yuan L, Seo JS, Kang NS, Keinan S, Steele SE, Michelotti GA, Wetsel WC, Beratan DN, Gong YD, Lee TH, Hong J. Identification of 3-hydroxy-2-(3-hydroxyphenyl)-4H-1-benzopyran-4-ones as isoform-selective PKC-zeta inhibitors and potential therapeutics for psychostimulant abuse. Mol. Biosyst. 2009; 5:927–930. [PubMed: 19668856]

52. Wu J, Zhang B, Wu M, Li H, Niu R, Ying G, Zhang N. Screening of a PKC zeta-specific kinase inhibitor PKCzI257.3 which inhibits EGF-induced breast cancer cell chemotaxis. Invest. New Drugs. 2009

53. Trujillo JI, Kiefer JR, Huang W, Thorarensen A, Xing L, Caspers NL, Day JE, Mathis KJ, Kretzmer KK, Reitz BA, Weinberg RA, Stegeman RA, Wrightstone A, Christine L, Compton R, Li X. 2-(6-Phenyl-1H-indazol-3-yl)-1H-benzo[d]imidazoles: design and synthesis of a potent and isoform selective PKC-zeta inhibitor. Bioorg. Med. Chem. Lett. 2009; 19:908–911. [PubMed: 19097791]

54. Whitson EL, Bugni TS, Chockalingam PS, Concepcion GP, Feng X, Jin G, Harper MK, Mangalindan GC, McDonald LA, Ireland CM. Fibrosterol sulfates from the Philippine sponge Lissodendoryx (Acanthodoryx) fibrosa: sterol dimers that inhibit PKCzeta. J. Org. Chem. 2009; 74:5902–5908. [PubMed: 20560563]

55. Pillai P, Desai S, Patel R, Sajan M, Farese R, Ostrov D, Acevedo-Duncan M. A novel PKC-iota inhibitor abrogates cell proliferation and induces apoptosis in neuroblastoma. Int. J. Biochem. Cell. Biol. 2011; 43:784–794. [PubMed: 21315177]

56. Stallings-Mann M, Jamieson L, Regala RP, Weems C, Murray NR, Fields AP. A novel small-molecule inhibitor of protein kinase Ciota blocks transformed growth of non-small-cell lung cancer cells. Cancer Res. 2006; 66:1767–1774. [PubMed: 16452237]

57. Sajan MP, Nimal S, Mastorides S, Acevedo-Duncan M, Kahn CR, Fields AP, Braun U, Leitges M, Farese RV. Correction of metabolic abnormalities in a rodent model of obesity, metabolic syndrome, and type 2 diabetes mellitus by inhibitors of hepatic protein kinase C-iota. Metabolism. 2012; 61:459–469. [PubMed: 22225955]

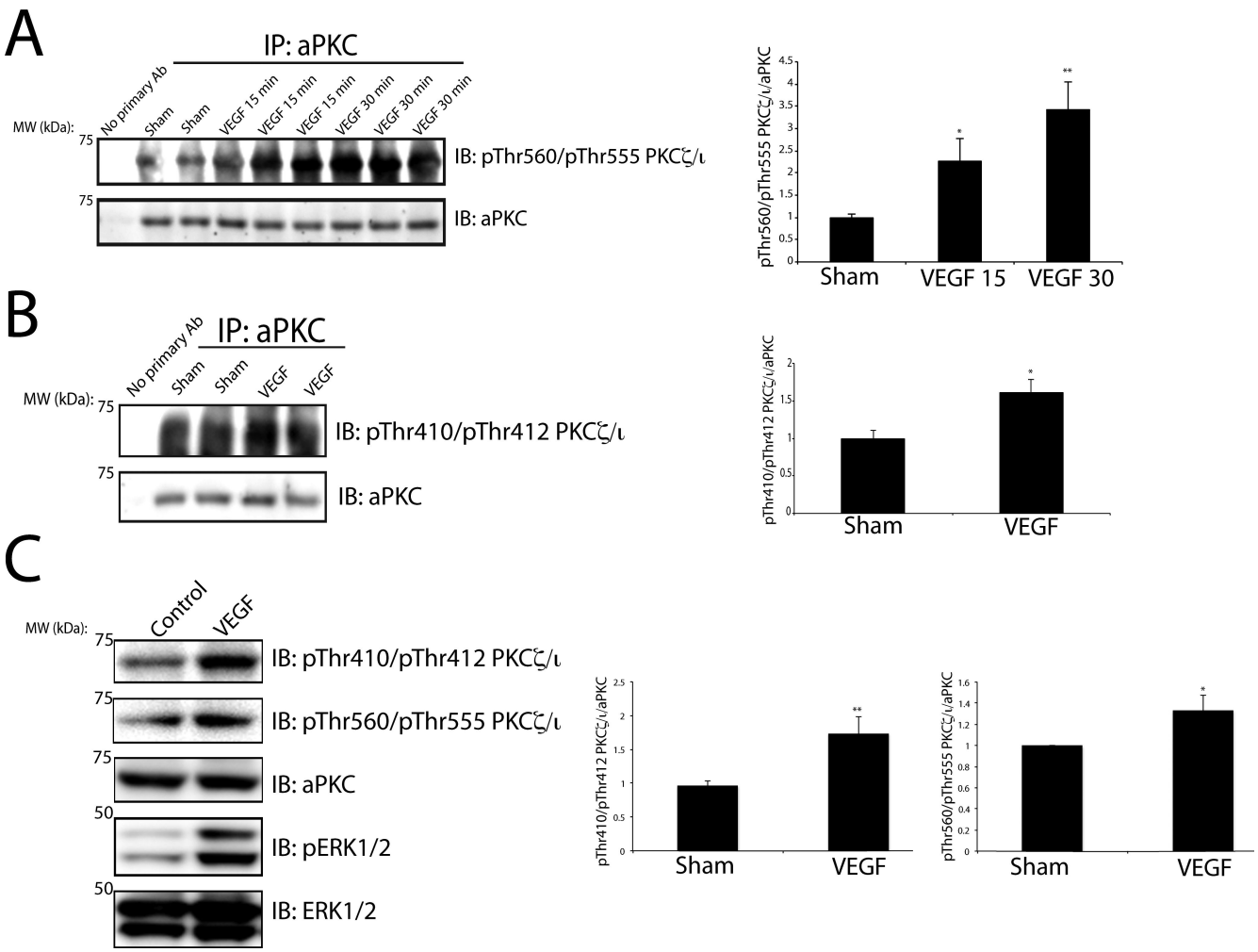

Fig. 1. VEGF activates aPKC isoforms in both the rodent retina and in primary retinal endothelial cells

(A) VEGF was intra-vitreally injected for the indicated time and retinas were excised from Sprague-Dawley rats. aPKC was immunoprecipitated where indicated and immunoblotted for the autophosphorylation residue, pThr560/Thr555. **(B)** VEGF was intra-vitreally injected for 15 min and retinas were excised from Sprague-Dawley rats. aPKC was immunoprecipitated where indicated and immunoblotted for the pThr410/Thr412. Successful immunoprecipiation was verified with immunoblotting for aPKC. Quantitation of the results (mean ± SEM) from three independent experiments and are expressed relative to the control with a total of n≥8. *, p<0.05, **p<0.01. **(C)** BREC were treated with VEGF (50 ng/ml) and lysates were subjected to immunoblotting for pThr410/Thr412 and pThr560/Thr555 PKCζ/ι, aPKC, pERK1/2, and ERK1/2 as described (methods). Quantitation of the results are expressed as the mean relative to the control, error bars represent ± SEM. n≥8. *, p<0.05, ** p<0.01.

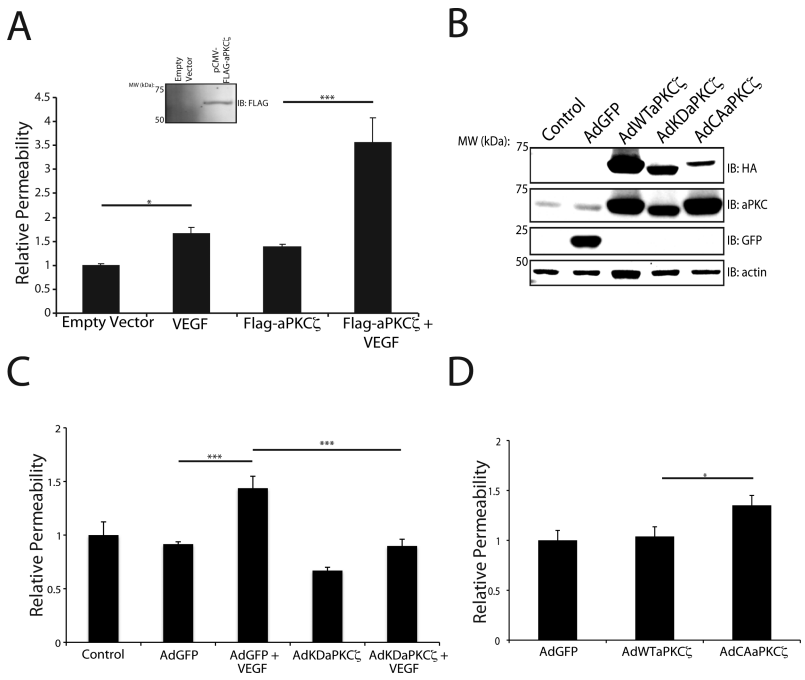

Fig. 2. aPKC kinase activity is both sufficient and required for VEGF-induced retinal endothelial permeability in primary culture

(A) Primary BREC were transfected with the plasmid pCMV-FLAG-aPKCζ or empty vector where indicated and grown to confluence on 0.4 μm Transwell filters.Immunoblot analysis utilizing Flag antibody showed successful expression of transgene. After 24 h serum deprivation, cells on filters were treated with 50 ng/ml VEGF as indicated. Permeability to 70 kDa RITC-Dextran tracer was measured over 4 hour time course. **(B)** BREC were transduced with recombinant adenoviruses and an immunoblot utilizing HA tag was performed to demonstrate successful transduction. Total aPKC content was monitored to demonstrate extent of transgene overexpression compared to control. **(C)** BREC were grown on transwells as above and infected with AdKDaPKCζ 6 h prior to a 24 h serum deprivation. Permeability to 70 kDa RITC-Dextran tracer was measured over 4 hour time course following VEGF treatment. **(D)** BREC were grown on transwells as above and infected with AdWTaPKCζ and AdCAaPKCζ. Permeability to 70 kDa RITC-Dextran tracer was measured over 4-hour time course following VEGF treatment. All results are expressed as the mean relative to the control with a total of n≥8, error bars represent ± SEM. Average Po values for Control and AdGFP were 2.0×10^{-6} (cm/s) and 1.47×10^{-6} (cm/s). ***, p<0.001 *, p<0.05.

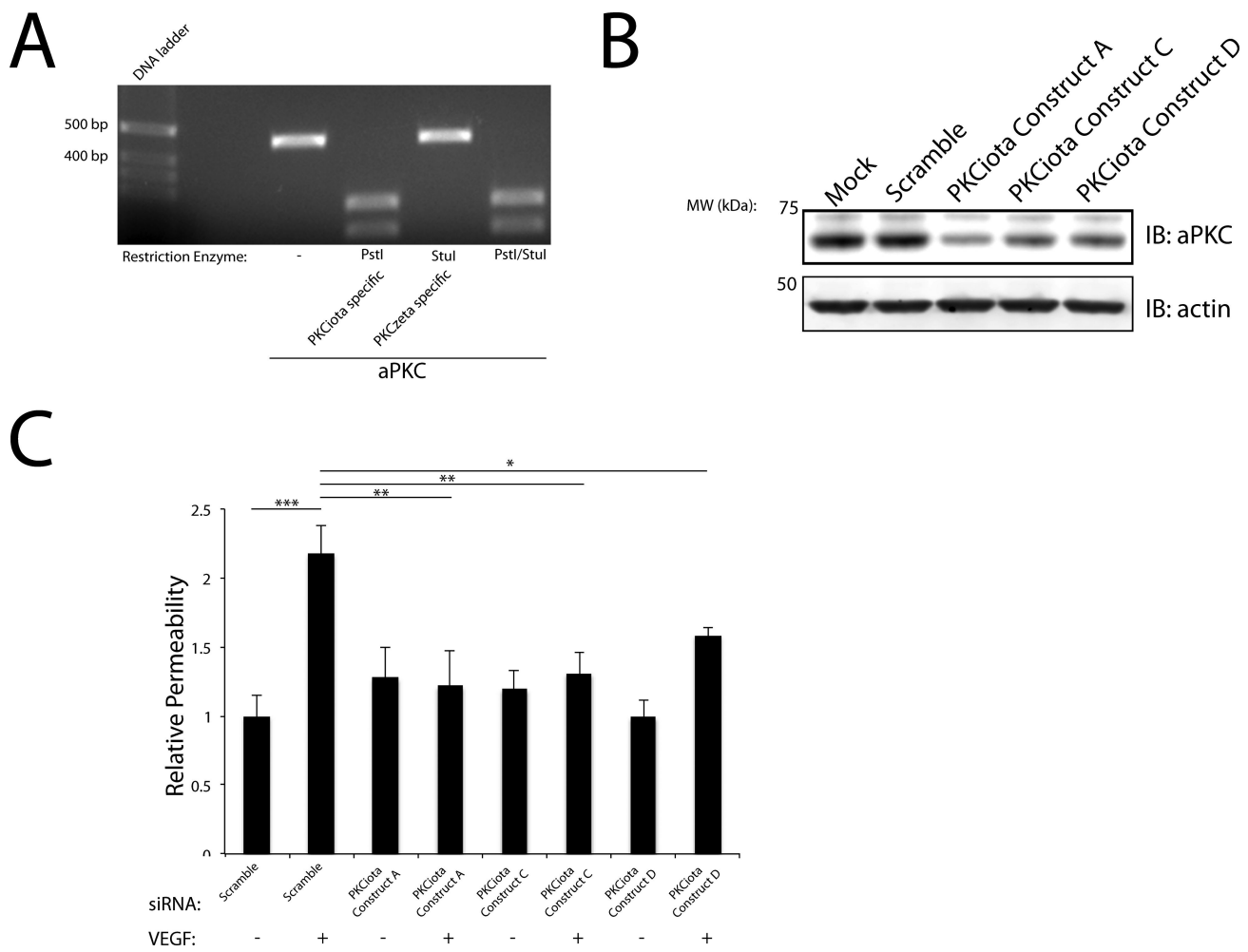

Fig. 3. PKCι mediates VEGF-induced retinal endothelial permeability in BREC

(A) PCR was performed using homologous primers for aPKCζ/ι that contained a unique restriction enzyme site to differentiate between the isoforms (Pst1 PKCι) and (Stu1 PKCζ). The amplicon generated was then subjected to restriction enzyme digestion. **(B)** BREC were transfected with either 100 nM Scramble or PKCι Constructs A/C/D and subjected to immunoblot analysis for aPKC. Actin served as a loading control. **(C)** BREC were transfected with either Scramble or with PKCι Construct A/C/D for 72 h. Permeability to 70 kDa RITC-Dextran tracer was measured over 4-hour time course following VEGF treatment. The results are expressed as the mean, relative to the control, error bars represent ± SEM. n≥3. Average Po values for Scr were 6×10^{-7} (cm/s) *, p<0.05, **,p<0.01, ***,p<0.001.

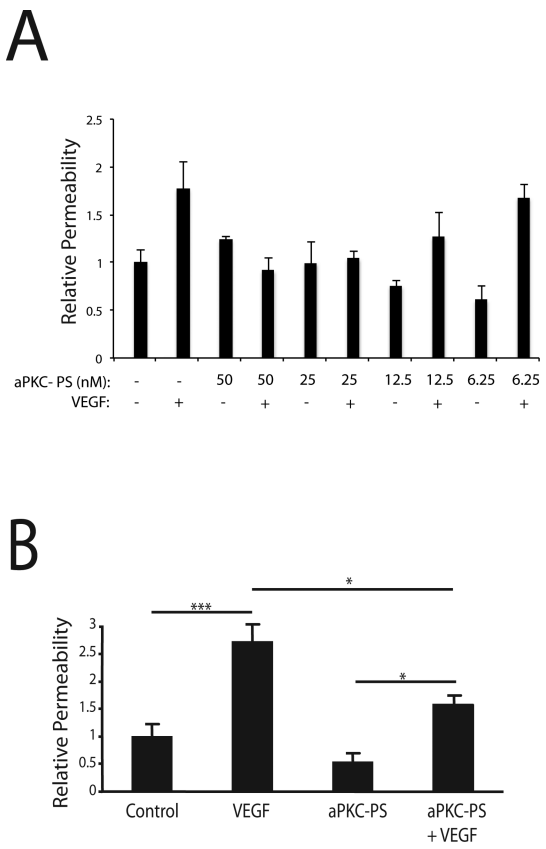

Fig. 4. aPKC peptide inhibitor blocks the VEGF-induced increase in endothelial permeability

(A) BREC were grown to confluence on 0.4 μm Transwell filters then stepped-down for 24 h. BREC were treated for 30 min with the indicated concentration of aPKC peptide inhibitor (aPKC-PS) prior to 30 min treatment with 50 ng/ml VEGF where indicated. Permeability of the monolayer to 70kDa RITC-Dextran was measured. n≥4. **(B)** BREC were treated with 50 nM aPKC peptide inhibitor for 30 min prior to 30 min treatment with 50 ng/ml VEGF. n≥4. Permeability was measured as in **(A).** The results are expressed as the mean relative to the control, error bars represent ± SEM. ***, $p<0.001$; *, $p<0.05$.

A

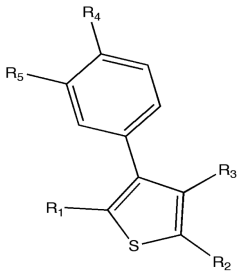

Chembridge ID #	R^1	R^2	R^3	R^4	R^5	IC_{50} (uM)
6131246	H	NH_2	$C_4H_6O_2$	Cl	Cl	7
6131706	H	NH_2	$C_4H_6O_2$	CH_3O	CH_3O	20
5132573	H	NH_2	$C_3H_5O_2$	F	H	26
5311310	H	NH_2	$C_3H_5O_2$	NO_2	H	41
5627112	H	NH_2	$C_3H_5O_2$	Br	H	28
n/a	H	NH_2	$C_3H_5O_2$	Cl	H	39
5632675	H	NH_2	$C_2H_3O_2$	Br	H	24
5635527	H	NH_2	$C_2H_3O_2$	H	H	62
n/a	H	NH_2	CO_2H	Cl	H	>100
n/a	H	C_2H_4NO	$C_3H_5O_2$	Cl	H	>100
n/a	H	C_2H_3O	C_2H_4NO	Cl	H	>100
n/a	H	$C_7H_4N_2O_3Cl$	$C_3H_5O_2$	Cl	H	>100
n/a	H	C_7H_4NOClF	$C_3H_5O_2$	Cl	H	>100
n/a	CH_3	NH_2	$C_3H_5O_2$	H	H	>100
n/a	CH_3	C_2H_4NO	$C_3H_5O_2$	H	H	>100
n/a	CH_3	C_2H_4NO	CO_2H	H	H	>100
7943464	CH_3	C_2H_4NO	$C_3H_5O_2$	CH_3O	H	>100
n/a	CH_3	$C_6H_{12}N_3O_2S_2$	$C_3H_5O_2$	H	H	>100
n/a	CH_3	$C_6H_4N_2O_3Cl$	$C_3H_5O_2$	H	H	>100
5634152	C_2H_4NO	C_2H_4NO	$C_3H_5O_2$	H	H	>100
n/a	C_2H_3O	C_2H_4NO	$C_3H_5O_2$	Cl	H	71
5218218	$C_5H_{10}N$	NH_2	$C_3H_5O_2$	H	H	>100

B

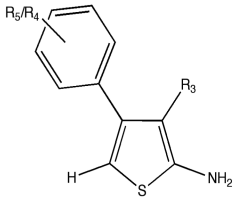

aPKC-I Pharmacophore

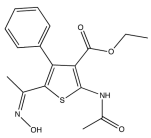

aPKC-I-PD

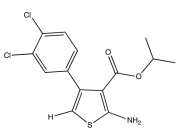

aPKC-I-diCl

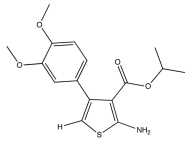

aPKC-I-diMeO

Fig. 5. Identification of novel, small molecule phenyl-thiophene inhibitors of aPKC isoforms

(A) Structure-activity relationships (SAR) were performed on phenyl-thiophene derivatives and IC_{50} determined using an *in* vitro luminescence based kinase assay against PKCζ using 200 ng/ml PKCζ, 25 uM CREBtide substrate, and 0.1 uM ATP. IC_{50} values were calculated using Prism Software with values fitted to a sigmoidal dose-response using variable slope. (n=6). **(B)** Pharmacophore of aPKC inhibitor noting essential substitutions and the structure of aPKC-I-PD, aPKC-I-diCl, and aPKC-I-diCl compounds are displayed where indicated. Compounds with Chembridge ID numbers (#) are provided and n/a (not applicable) applies to compounds synthesized in collaboration with Apogee, Inc. (methods).

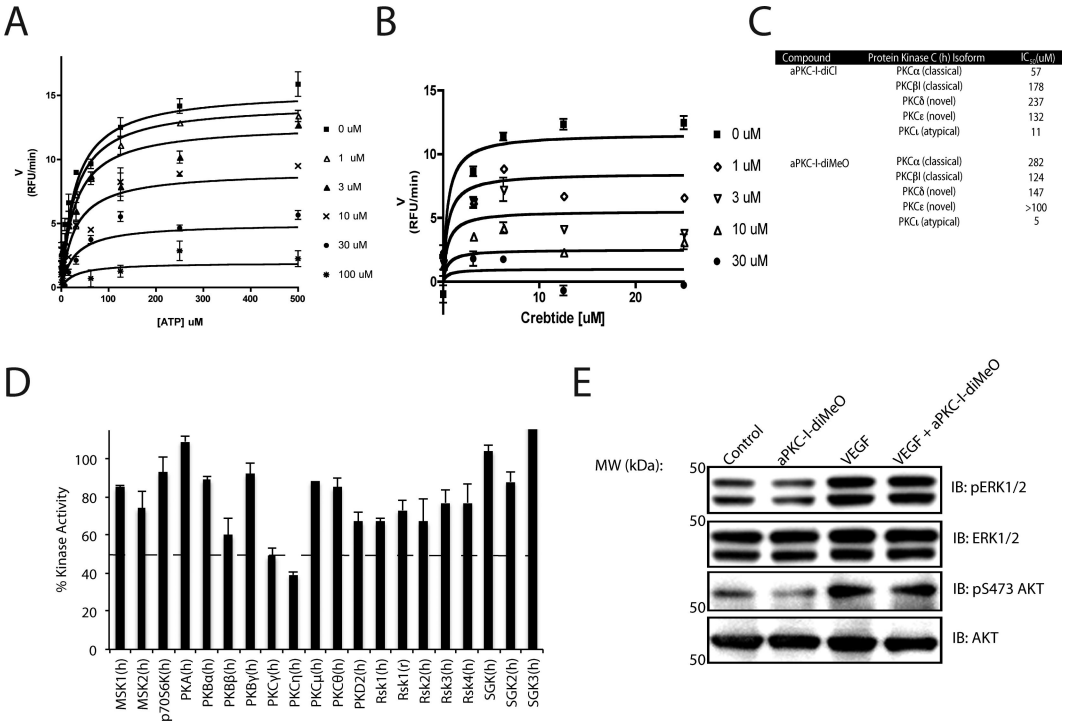

Fig. 6. Mechanism of action and specificity characterization of aPKC-Is

(A) ATP competition assay using ADP quest to measure initial velocities with 500 ng/ml PKCζ and excess CREBtide substrate or **(B)** with excess ATP. K_i was determined as described in methods. **(C)** IC_{50} profiling was performed with aPKC-I-diCl and aPKC-I-diMeO utilizing a radiolabeled kinase assay at K_m app for ATP. **(D)** aPKC-I-diMeO at 100 uM (10-fold K_i) was screened against 20 kinases of the AGC super-familiy at K_m app for ATP using a radiolabeled kinase assay. **(E)** BREC were pretreated for 30 min with 0.3 uM aPKC-I-diMeO and then stimulated with VEGF (50ng/ml) for 15 min. Lysates were subjected to immunoblotting for pERK1/2, ERK1/2, pS473-AKT, and AKT as described (methods).

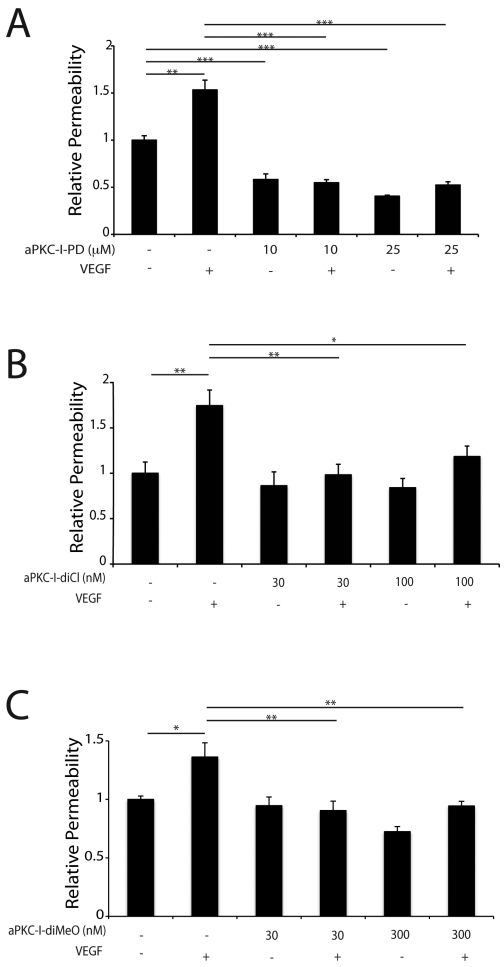

Fig. 7. Phenyl-thiophene inhibitors of aPKC isoforms prevent VEGF-induced retinal endothelial permeability in primary culture

BREC were grown to confluence on 0.4 μm Transwell filters then serum deprived for 24 h. **(A)** BREC were treated for 30 min with aPKC-I-PD **(B)** or aPKC-I-diCl **(C)** or aPKC-I-diMeO prior to 30 min treatment with 50 ng/ml VEGF where indicated. Permeability of the monolayer to 70kDa RITC-Dextran was measured. The results are expressed as the mean relative to the control with a total of n≥8, error bars represent ± SEM. Average Po value in **(A)** was 2.43×10^{-6} (cm/s), **(B)** 2.49×10^{-7} (cm/s) and **(C)** 1.46×10^{-6} (cm/s). ***, p<0.001; **, p<0.01; *, p<0.05.

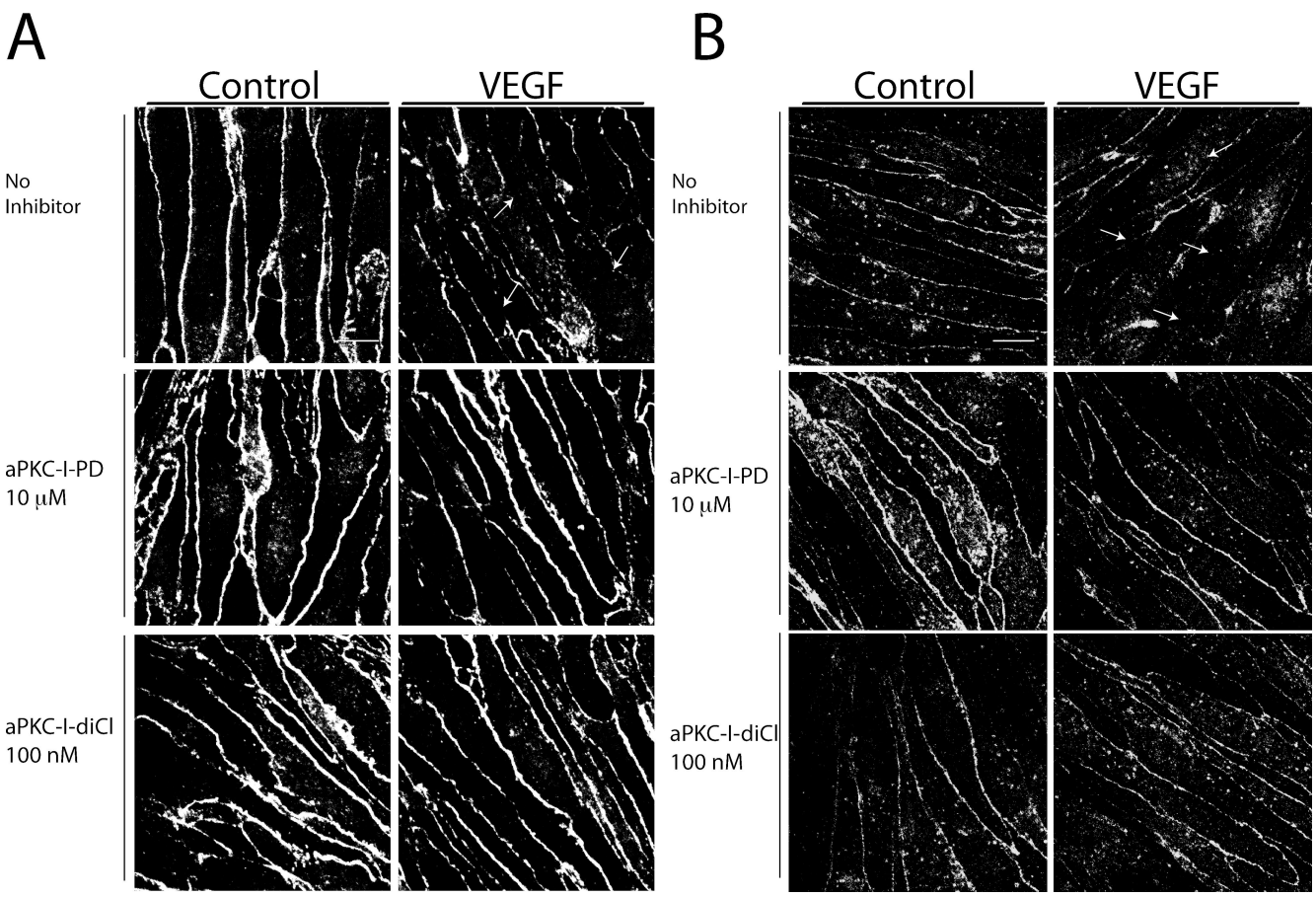

Fig. 8. Novel small molecule inhibitors of aPKC isoforms prevent the effect of VEGF on breakdown of the retinal endothelial tight junction complex

BREC were grown to confluence on coverslips and treated with 10 μM aPKC-I-PD, or 100 nM aPKC-I-diCl 30 min prior to 50 ng/ml VEGF. Cells were fixed 60 min after VEGF treatment and stained with primary antibodies against **(A)** ZO-1 or **(B)** occludin. Cells were imaged with confocal microscopy and are shown as the max projection of serial stacks. Images are representative of several similar fields. Scale bar = 10 μm.

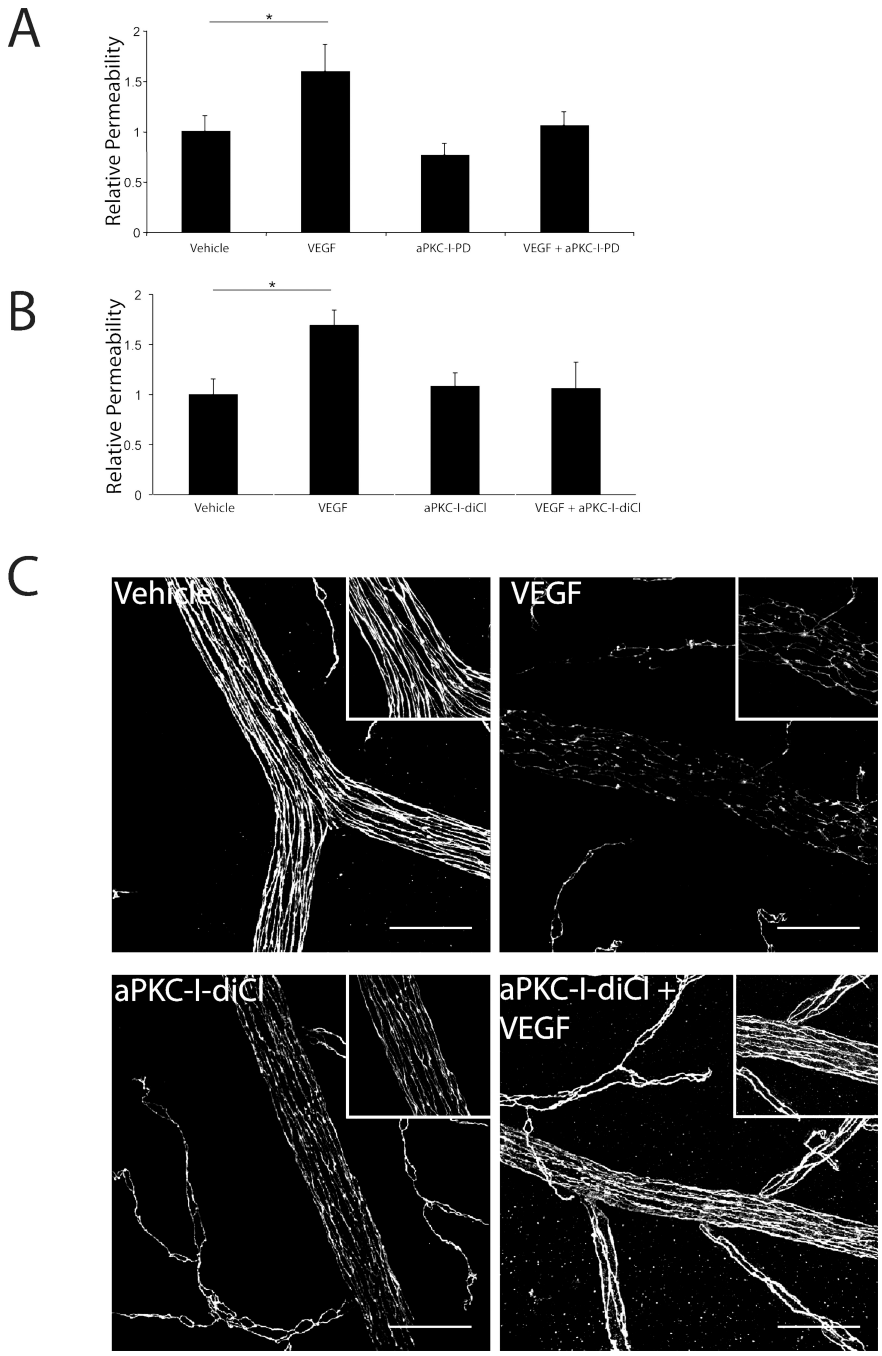

Fig. 9. aPKC-Is block the VEGF induction of retinal vascular permeability *in vivo*

Sprague-Dawley rats were injected intra-vitreally with **(A)** aPKC-I-PD at 25 μM or **(B)** aPKC-I-diCl at 25 μM with or without 50 ng VEGF per eye and compared to vehicle injection. After 3 h, rats received a femoral vein injection of 45 mg/kg Evans blue. After 2 h, animals were perfused with citrate/paraformaldehyde buffer for 2 min, retinas removed, dried and Evans blue extracted with formamide. Evans blue was quantified on a spectrophotometer and normalized to plasma levels measured pre-perfusion. Permeability was calculated and expressed as μl plasma/g dry weight/h circulation. The results are expressed as the mean relative to the control, error bars represent ± SEM. n≥8 per group, * $p<0.05$. **(C)** Retina flat mounts were prepared as described in Materials and Methods and

immuno-stained for occludin. Images are representative of several fields and are shown as the max projection of serial stacks obtained from confocal imaging. Scale bar = 50 μm.